CONF-9505105--7

GA-A22039

FAST WAVE CURRENT DRIVE ON DIII-D

by

J.S. deGRASSIE, C.C. PETTY, R.I. PINSKER, C.B. FOREST, H. IKEZI, R. PRATER, F.W. BAITY, R.W. CALLIS, W.P. CARY, S.C. CHIU, E.J. DOYLE, S.W. FERGUSON, D.J. HOFFMAN, E.F. JAEGER, K.W. KIM, J.H. LEE, Y.R. LIN-LIU, M. MURAKAMI, R.C. O'NEILL, M. PORKOLAB, T.L. RHODES, and D.W. SWAIN

JUNE 1995

GENERAL ATOMICS

DISCLAIMER

GA–A22039

FAST WAVE CURRENT DRIVE ON DIII–D

by

J.S. deGRASSIE, C.C. PETTY, R.I. PINSKER, C.B. FOREST, H. IKEZI, R. PRATER, F.W. BAITY,* R.W. CALLIS, W.P. CARY, S.C. CHIU, E.J. DOYLE,† S.W. FERGUSON,‡ D.J. HOFFMAN,* E.F. JAEGER,* K.W. KIM,† J.H. LEE,† Y.R. LIN-LIU, M. MURAKAMI,* R.C. O'NEILL, M. PORKOLAB,♯ T.L. RHODES,† and D.W. SWAIN*

This is a preprint of an invited paper presented at the 11th Topical Conference on Radio Frequency Power in Plasmas, May 17–19, 1995, Palm Springs, California, and to be printed in the *Proceedings.*

Work supported by U.S. Department of Energy
Contracts DE–AC03–89ER51114, DE–AC05–84OR21400,
DE–FG03–86ER53225, and W–7405–ENG–48

* Oak Ridge National Laboratory
† University of California, Los Angeles
‡ Lawrence Livermore National Laboratory
♯ Massachusetts Institute of Technology

GENERAL ATOMICS PROJECT 3466
JUNE 1995

Fast Wave Current Drive on DIII–D

J.S. deGrassie, C.C. Petty, R.I. Pinsker, C.B. Forest, H. Ikezi, R. Prater, F.W. Baity,* R.W. Callis, W.P. Cary, S.C. Chiu, E.J. Doyle,† S.W. Ferguson‡ D.J. Hoffman,* E.F. Jaeger,* K.W. Kim,† J.H. Lee,† Y.R. Lin-Liu, M. Murakami,* R.C. O'Neill, M. Porkolab,♯ T.L. Rhodes,† and D.W. Swain,*

General Atomics, San Diego, California 92186
**Oak Ridge National Laboratory, Oak Ridge, Tennessee 37831*
†University of California, Los Angeles, California 90024
‡Lawrence Livermore National Laboratory, Livermore, California 94551
♯Massachusetts Institute of Technology, Cambridge, Massachusetts 20139

Abstract. The physics of electron heating and current drive with the fast magnetosonic wave has been demonstrated on DIII–D, in reasonable agreement with theoretical modeling. A recently completed upgrade to the fast wave capability should allow full noninductive current drive in steady state advanced confinement discharges and provide some current density profile control for the Advanced Tokamak Program. DIII–D now has three four-strap fast wave antennas and three transmitters, each with nominally 2 MW of generator power. Extensive experiments have been conducted with the first system, at 60 MHz, while the two newer systems have come into operation within the past year. The newer systems are configured for 60 to 120 MHz. The measured FWCD efficiency is found to increase linearly with electron temperature as $\gamma = 0.4 \times 10^{18}\, T_{e0}$ (keV) [A/m^{2}W], measured up to central electron temperature over 5 keV. A newly developed technique for determining the internal noninductive current density profile gives efficiencies in agreement with this scaling and profiles consistent with theoretical predictions. Full noninductive current drive at 170 kA was achieved in a discharge prepared by rampdown of the Ohmic current. Modulation of microwave reflectometry signals at the fast wave frequency is being used to investigate fast wave propagation and damping. Additionally, rf pick-up probes on the internal boundary of the vessel provide a comparison with ray tracing codes, with clear evidence for a toroidally directed wave with antenna phasing set for current drive.

There is some experimental evidence for fast wave absorption by energetic beam ions at high cyclotron harmonic resonances.

INTRODUCTION

The DIII–D program is focused upon demonstrating the physics basis for an advanced performance tokamak reactor, with advanced performance defined by enhanced confinement and stability limits [1,2]. The assumption is that advanced regimes achieved transiently on DIII–D will be realized for steady state with the development of full control of the noninductive current density profile. One key tool in this effort on DIII–D is current drive with fast magnetosonic waves, so called fast wave current drive (FWCD). The fast wave is projected to have excellent penetration and absorption in a hot dense reactor core, capable of efficient central current drive. As a key step in the validation of FWCD, DIII–D is committed to a demonstration of total noninductive current drive with a relaxed current density profile.

FWCD provides a means for control of the current density profile for advanced tokamak discharge development. Following encouraging results in high β_p discharges [3], FWCD will be tested for control of the safety factor on axis $q(0)$ with central current drive in a feedback mode. In another scenario, discharges with high internal inductance, produced by transient techniques, have been shown to have enhanced confinement [4,5]. The central current drive resulting from FWCD should provide a steady-state route to this "high-ℓ_i" scenario. Off axis current drive may be produced through mode conversion current drive (MCCD), a mechanism receiving considerable attention at this time [6,7]. This would allow control of the minimum value of the safety factor off axis q_{min} in reversed central shear discharges [1,2].

In the past few years the physics of FWCD and fast wave electron heating has been established on DIII–D [8–10]. Using a single four-strap antenna [11,12] the technological difficulties of launching a directed spectrum with a single 2 MW, 60 MHz, rf generator have been overcome [13] and FWCD and heating efficiencies in good agreement with theoretical code calculations have been obtained [9,14]. For the DIII–D system parameters, the efficiency increases linearly with central electron temperature, and it projects favorably to achievement of the steady state noninductively driven discharge. The electron heating deposition profile has been measured with the power modulation technique, also agreeing with theoretical calculations. Transiently, full noninductive current drive has been obtained on DIII–D with this fast wave system coupled with additional heating via electron cyclotron heating [8].

Recently two additional FWCD systems have been brought into operation on DIII–D. Each system comprises a four-strap antenna and a 2 MW rf generator [15,16]. These new systems are presently configured to operate over the 60 to 120 MHz range. This higher frequency range requires that the straps be folded in the poloidal direction to optimize the rf current distribution in the strap. Initial experiments with these systems have also demonstrated electron heating and current drive commensurate with the theoretical calculations. Recently a powerful analysis technique has been developed and validated which allows an unfolding of the noninductive current density profile from kinetic profile data and calculated equilibria [17]. The FWCD profile measured in this manner also agrees with theoretical predictions.

An effort is now underway to fully integrate all three FWCD systems into routine DIII–D operation for execution of the advanced tokamak program. Maintaining a continuous match to the dynamic loading (ELMs) encountered in some advanced confinement regimes will require new approaches. One potential solution to the dynamic nature of the plasma load is high power ferrite tuner systems [18]. A prototype ferrite tuner will be tested on DIII–D next year. Another potential solution is the use of a novel antenna, a combline antenna [19], which is far more tolerant of plasma load variations than a conventional strap antenna. Low power measurements of a combline configuration on DIII–D are promising in this regard [20].

The advanced tokamak scenarios also make use of neutral beam heating. Experiments and calculations [21] are in progress to assess the level of direct absorption of fast waves by the high energy beam deuterons, which will occur at high harmonics of the gyrofrequency for the DIII–D parameters ($B_T < 2.1$ T). This absorption mechanism would compete with FWCD.

As part of understanding the physics of fast waves in DIII–D, new diagnostics have been brought to bear to make measurements of the waves within the plasma and on the boundary. Analysis of data from rf $\partial B/\partial t$ probes on the boundary has shown that the CURRAY ray tracing code is accurate at least for the first toroidal transit of the wave [22], limited so far by the ability to unfold the probe signals for greater wave transits. Microwave reflectometry has been used to measure the rf density fluctuation within the plasma driven by the launched fast wave [23]. Both of these diagnostics reveal the directivity of the fast wave with appropriate phasing of the antenna straps. Reflectometry is also used to measure the edge density profile [24], which is used to compute the theoretical rf loading of an antenna. These loading calculations are in agreement with experiment.

DIII-D FAST WAVE SYSTEMS

The outer midplane locations of the three fast wave antennas are indicated in Fig. 1. The first antenna (F1) has been used in many experimental campaigns, with a variety of Faraday shield configurations, including two tests with no shield [25]. The other two antennas (F2A and F2B) are identical and were installed in 1994. Details of the antenna designs are given elsewhere [11,16], as well as the transmission systems [13,15]. Spectral calculations have been performed with the RANT3D code [26]. Figure 1 also indicates the location of the rf pick up probes and the microwave reflectometers.

The Faraday shield rods for all antennas are slanted at 12 deg relative to the midplane as shown in Fig. 1, to better match the magnetic field line pitch at the shields [27]. All plasma facing wall surfaces on DIII-D are armored with graphite tiles which provide protection for the Faraday shields which are situated 1 to 2 cm behind the surface of the tiles at the outer midplane.

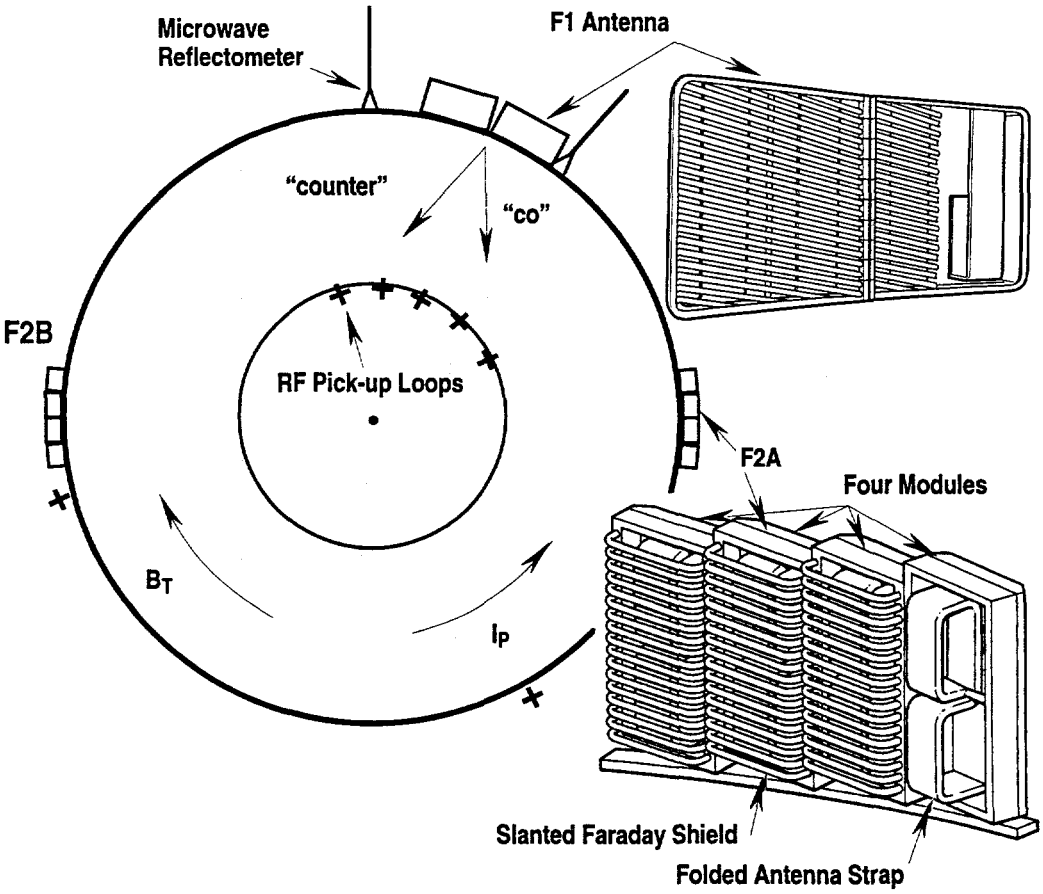

FIGURE 1. Layout of DIII-D showing the location of the F1 and two F2 antennas, the rf pick up probes, and the reflectometer horns.

All shields have the plasma facing sides coated with boron carbide, although the F1 antenna has been operated for some experiments with no shield at all, and also with no boron carbide coating on the shield, that is, the inconel substrate facing the plasma. The boron carbide coatings have performed satisfactorily provided that the coating is thin enough ($<\sim 100$ μm). Thicker coatings cracked and eroded during plasma operation, apparently due to lack of thermal contact to the base shield rod material. DIII–D routinely uses boronization for wall conditioning [28].

The rf transmission and matching systems on DIII–D utilize resonant loops, mechanical phase shifters, and stubs for tuning and decoupling [15]. The F1 system has been operated at 60 MHz, while the F2 systems have been operated at several frequencies between approximately 60 and 90 MHz. The newer systems are in the process of being brought to full capability [29].

FWCD RESULTS ON DIII–D

Experiments on DIII–D have verified the theoretical predictions for FWCD. These experiments have been done in a relatively high frequency range, from 4 to 10 times the deuterium ion gyrofrequency on axis, to minimize competition from resonant ion absorption. The two newer systems were also selected to have their high frequency capability in order to minimize the damping length of the fast wave in the first pass across the plasma [30], thereby gaining greater current drive on the first pass. However, the experiments have shown that multipass absorption is effective for electron heating and current drive, except in the most extreme parameter regime of very weak damping [8]. That is, to obtain agreement with theory, credit must be taken for multipass interactions.

A summary of the FWCD efficiencies measured in DIII–D from many experiments is shown in Fig. 2, plotted versus the central electron temperature [8]. The dotted lines give the prediction of the CURRAY code [31] for the experimental parameters. The circles are based upon measurements of the loop voltage reduction below that predicted by the ONETWO transport code [32], while the diamonds are from a determination of the fast wave current profiles [33]. A phenomenological edge loss of 4% is included in CURRAY to match the efficiencies at $B_T = 1$ T [8]. Projection of these efficiencies to higher electron temperature results in FWCD in agreement with the previous "intermediate" and "long-term" fully noninductive DIII–D scenarios [30], which require ECH for electron preheating.

Complete noninductive current drive has been achieved transiently in DIII–D discharges with the F1 system coupled with approximately 1 MW

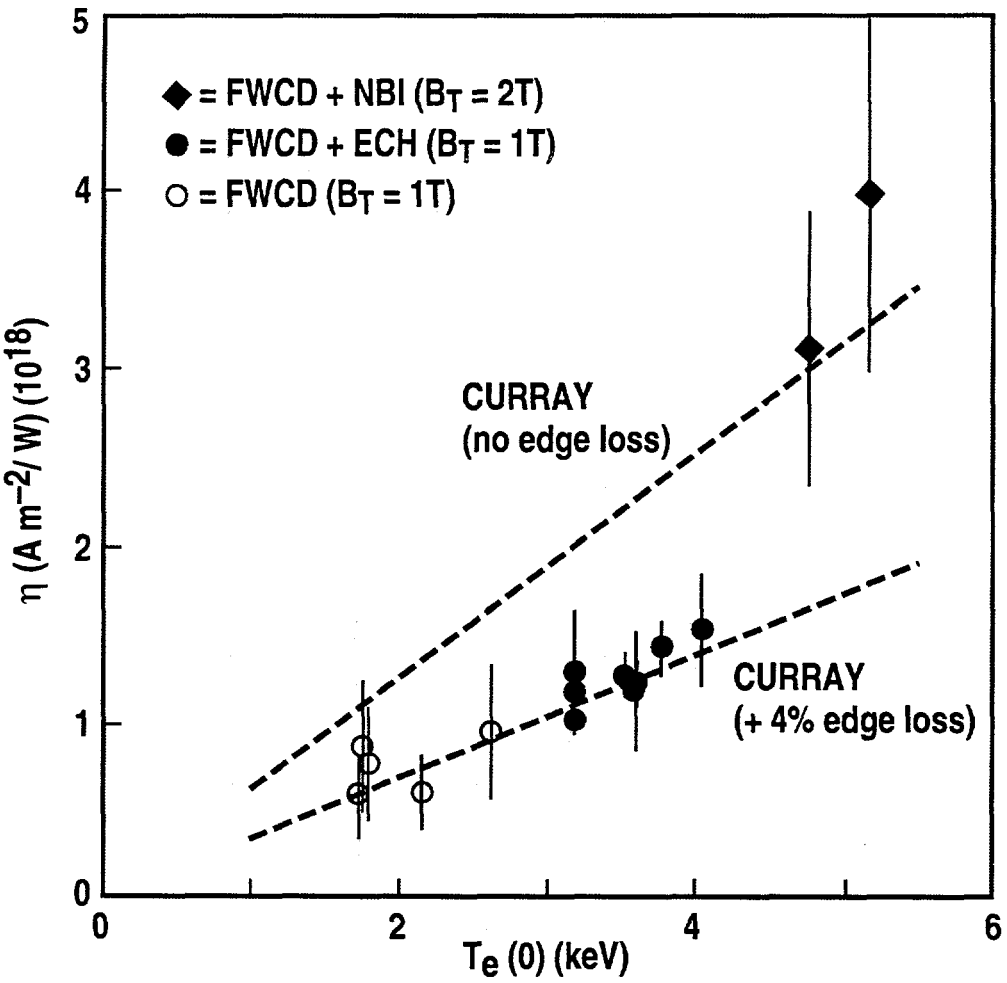

FIGURE 2. Summary of measured DIII-D FWCD efficiency versus $T_e(0)$.

of 60 GHz second harmonic electron cyclotron heating [8]. These discharges were prepared by rapidly ramping down the plasma current which results in a transient state of enhanced normalized energy confinement [5]. Time traces from such a discharge are shown in Fig. 3. ECH and FWCD are applied just before the rampdown. The Ohmic heating power supply operates in a standard feedback mode by varying the loop voltage V_L to follow the programmed plasma current I_p. The loop voltage analysis technique reveals a reduction in V_L below that predicted without any rf current drive between 2700 and 2800 msec in the discharge, as indicated by the ONETWO predicted points. With the F1 antenna symmetrically phased there is no reduction in V_L below that predicted, as expected for nondirectional waves, and indeed V_L is positive for the comparison discharge. For this FWCD discharge $I_p = 170$ kA, the bootstrap current is calculated to be $I_{BS} = 60$ kA, the EC driven current (the launch direction creates a nonzero parallel wavenumber)

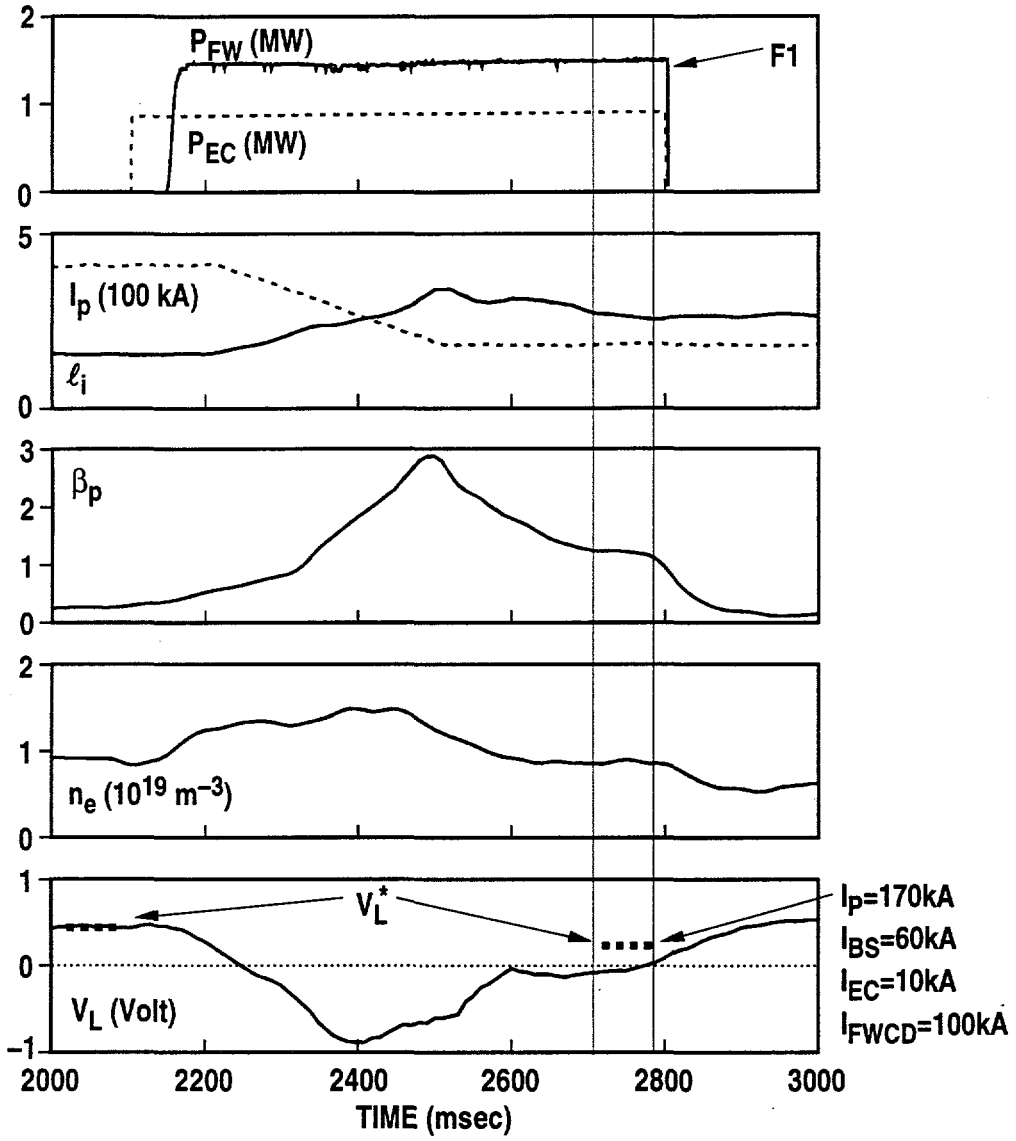

FIGURE 3. Transient full noninductive current drive achieved with FWCD (F1) and second harmonic ECH (60 GHz), $B_T = 1.1$ T. The rf current drive is evident by the reduction in the loop voltage V_L below that from simulation V_L^*.

is calculated to be $I_{ECCD} = 10$ kA and a lower limit on the FWCD is deduced to be $I_{FWCD} = 100$ kA.

An experimental determination of the noninductive current density profile has been made for FWCD discharges. This determination is accomplished with Forest's method [17] of computing the difference between the total current density profile, obtained from an equilibrium reconstruction incorporating measurements of the internal poloidal magnetic field, and

the Ohmic current density profile. This Ohmic profile is calculated from the inductive electric field obtained from the time derivative of successive equilibria and using kinetic measurements to determine the conductivity profile.

The FW current profile determined in this manner for one extensively studied case is shown in Fig. 4, along with three theoretical predictions [33]. In this discharge, both the F1 and F2A (at 89.6 MHz) antennas were used for FWCD. All four profiles are calculated with no free parameters. The quantitative agreement is very good. The theoretical calculations were performed using CURRAY, the reduced full wave code PICES [26], and the FASTCD code which is based upon an ergodicized wave density distribution in k space [34]. In Fig. 2, the diamond symbols identify the computed efficiencies for these profile data and those from another discharge.

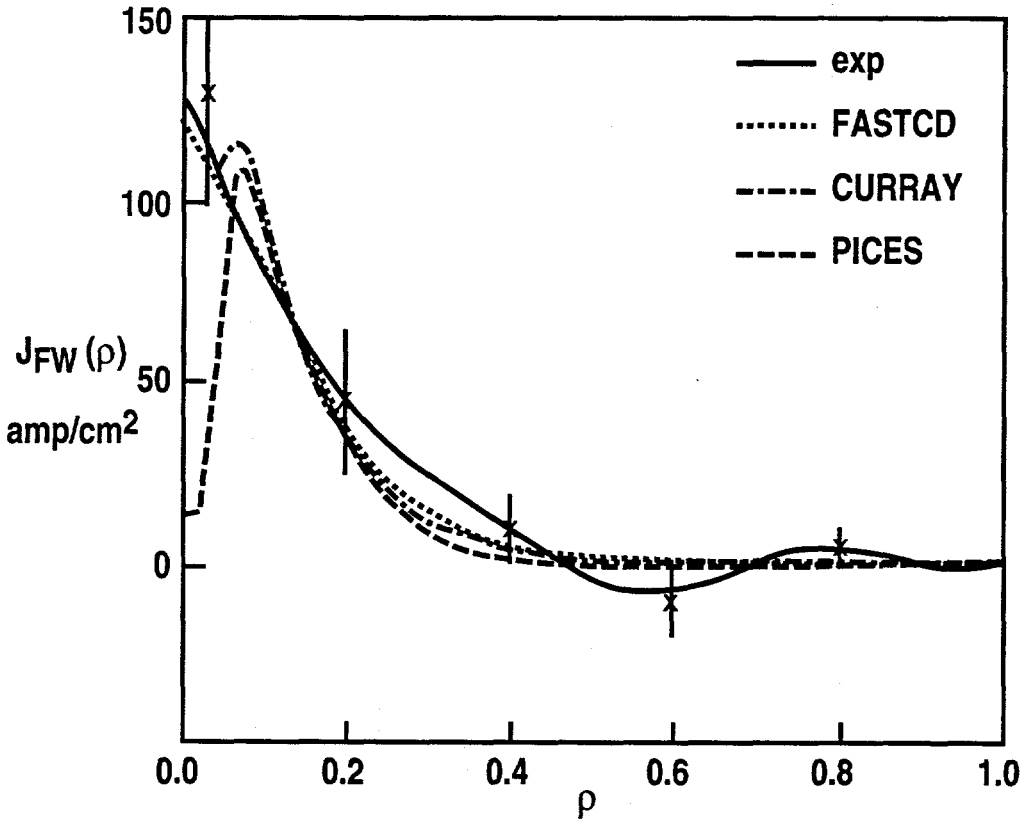

FIGURE 4. Comparison of FWCD spatial profile with three theoretical models. $I_p = 1.4$ MA, $I_{FW} = 135$ kA, $T_e(0) = 4.5$ keV, $n_{e0} = 2.9 \times 10^{19}/m^3$, $B_T = 2.1$ T, $P_{NB} = 3.5$ MW, $P_{FW} = 1.4$ MW.

WAVE PROPAGATION MEASUREMENTS

The rf pick-up loops indicated in Fig. 1 have been used extensively to study the fast waves received at these locations, and to demonstrate directionality of propagation consistent with the phasing of an antenna [22]. One example of this directionality is shown in Fig. 5 where Fourier analysis of data from the inner wall probe array is used to extract the parallel wavenumber of the fast wave launched by the F1 antenna at 60 MHz. Contours of constant received power are shown as a function of $k_{\|}$ and time throughout a shot. Data from three separate discharges are shown, and the strength of the received power varies depending upon the evolution of the shot. The relative rf phasing of the straps with increasing toroidal angle is indicated for each case. In (a) the antenna phasing was monopole and the spatial power spectrum is peaked about $k_{\|} = 0$, as expected. In (b) and (c) the antenna phasing is set for counter, and co, current drive directionality, respectively, and $k_{\|}$ changes sign between the two cases, with the spectrum centered approximately about $|k_{\|}| \cong 4\pi$ m^{-1}. In comparison with spectral computations, we find that some upshift of the wavenumber has occurred due to propagation to smaller major radius, but detailed data analysis reveals the upshift to be smaller than expected from geometrical considerations [22].

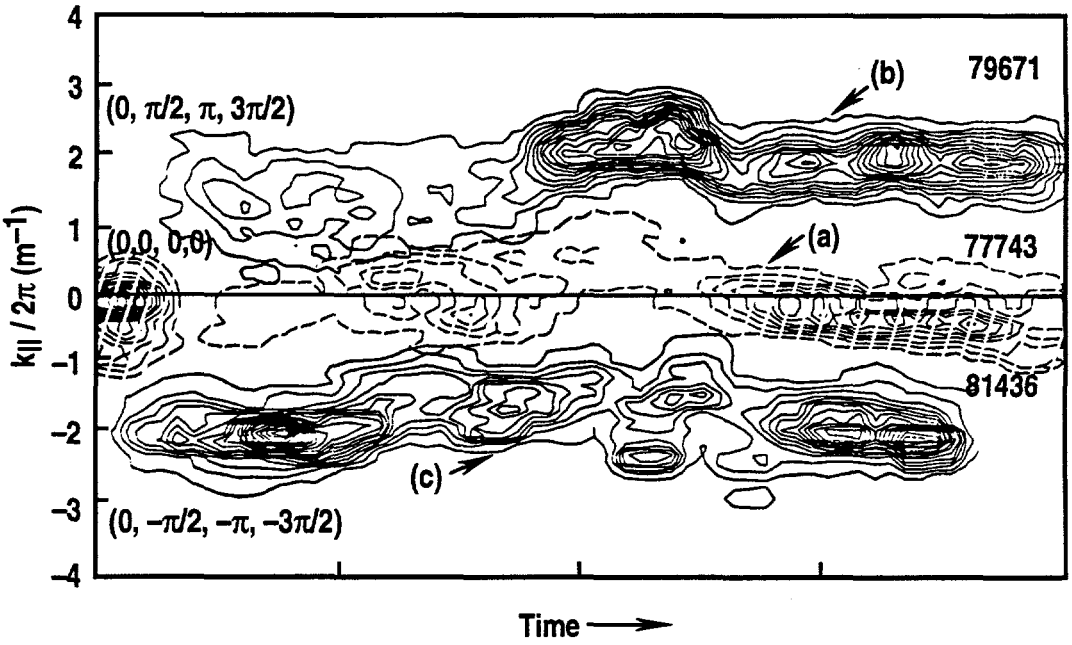

FIGURE 5. Wavenumber determination from the inner rf probe array reveals fast wave directionality with phased F1 antenna. Typical data from three distinct, and different, discharges.

Microwave reflectometry measurements of the spatially localized wave-coherent internal fluctuations of the electron density also indicate directionality [23]. The reflectometry system adjacent to the F1 antenna shows this most clearly. Figure 6 displays data from this system in front of the reflectometry horns near the edge of this antenna. The co-current drive case launches a wave which passes promptly in front of the measurement volume and thus produces a larger wave amplitude response than the counter-case wherein the dominant lobe of the wave spectrum must pass at least once around the torus before entering this volume.

FAST WAVE CURRENT DRIVE FOR ADVANCED TOKAMAK SCENARIOS

These experiments give confidence in the computational tools used to model FWCD and that the physical picture is correct. In the course of future experiments these models will continue to be refined. DIII-D now has the necessary FW system for the AT program, and in the future will reacquire an ECH system to complete the rf capability [30]. With the FW system alone, DIII-D should be able to demonstrate sustained full noninductive current drive, and examine the possibility of local current density profile control.

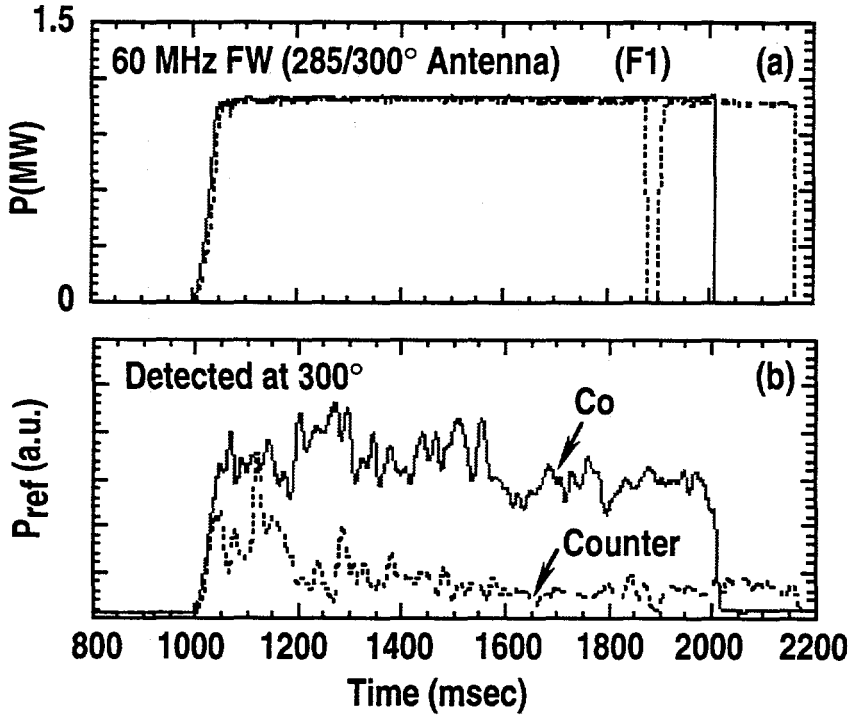

FIGURE 6. Fast wave coherent reflectometer signal for co and counter current drive phasing. (a) F1 power for two shots, (b) detected reflectometer power.

Central FWCD is used in high-ℓ_i simulated AT discharges for DIII–D. The profiles for one such 1 MA discharge are shown in Fig. 7, together with the simulated parameters. All current is driven noninductively. This computation was performed self-consistently with ONETWO in the coupled equilibrium and transport mode, taken to a steady-state condition. FWCD is calculated with CURRAY using extrapolated efficiencies consistent with those obtained on DIII–D. No wave damping on beam ions is considered. The present DIII–D FW systems can provide the required amount of power coupled to the plasma, used in this simulation. This case is significant in that it projects a continuous discharge with simultaneously good confinement H and normalized stored energy β_n, without any development other than high time averaged coupling of fast waves to potentially ELMing discharges. However, the H β_n factor is projected to be much larger for the so-called Second Stable Core VH–mode scenario [2]. Fast wave electron heating is used for this latter scenario, but not current drive, rather ECCD is the baseline approach to providing the necessary off-axis current drive for this reversed central shear profile case.

One promising method for using fast waves for off-axis current drive is MCCD, in which the fast wave is mode converted to the slow ion Bernstein wave in a two-ion species plasma, at a radial position determined by the ratio of the species mix and their gyrofrequencies. Tests of MCCD can be done on DIII–D with all FW systems operating near the lower end of the frequency band of the transmitters.

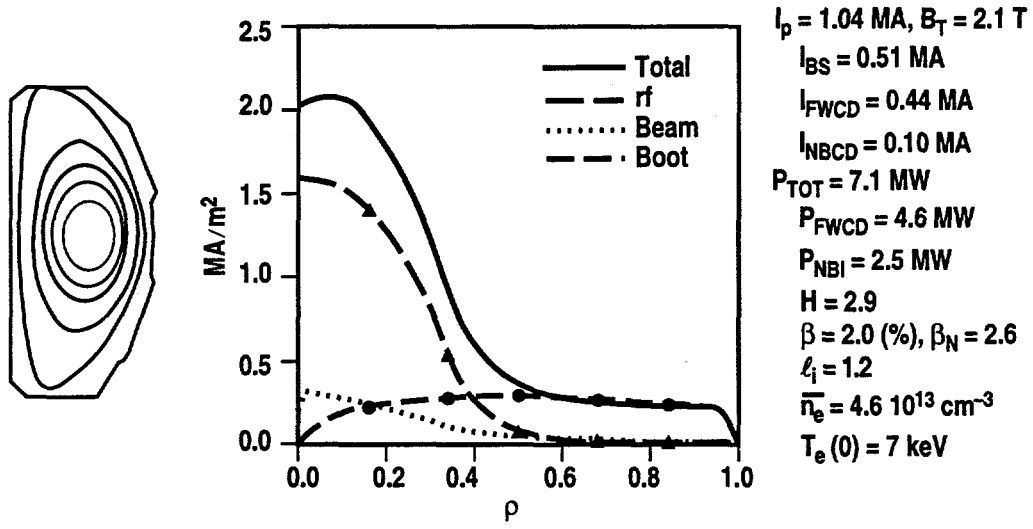

FIGURE 7. High ℓ_i simulated AT scenario on DIII–D using FWCD.

ADVANCED COUPLING TECHNIQUES

Experience on DIII–D indicates that advanced coupling techniques will be required to efficiently couple fast wave power to enhanced performance discharges due to the dynamic nature of the plasma load encountered. Such techniques must make possible high duty cycle mating of the generator power to the plasma, that is, providing an efficient match and minimal generator interruption for protection against high reflection events. As is well known from experience, any automatic matching scheme must be integrated with a reliable arc detection system to guard against matching the generator to an arc in the transmission line or antenna [35].

Two such advanced coupling techniques are being explored on DIII–D. First, a high power matching element based upon phase shifts in variable phase velocity ferrite loaded lines, rather than mechanically movable parts, will be tested. This Fast Ferrite Tuner (FFT) [18] should be capable of following load excursions down to the millisecond timescale. A low power test of a FFT system on DIII–D in the past demonstrated the potential for fast matching [36].

Second, low power tests of a type of combline antenna on DIII–D have shown this antenna to have exceptional insensitivity to changes in the plasma load, while coupling a sufficient fraction of the incident power to the plasma [20]. The principle of the combline concept is to use mutual coupling between adjacent straps to create a traveling wave along the antenna which is damped by radiation into the plasma. In the original form the coupling is internal to the vacuum vessel, reducing the number of required rf feeds through the vessel wall [19]. The coupling can also be external [20,37]. One of the four-strap F2 antennas was reconfigured for low power combline tests using external inductive coupling. Power was fed in at one end strap and that not radiated was absorbed in a load at the other end.

The coupling insensitivity of this F2 combline to plasma conditions is demonstrated by the traces in Fig. 8. The D_α trace delineates the Ohmic (Ω) and H–mode phases, with ELMs, and the no-plasma condition (VAC) after discharge termination. The power reflected to the generator remains small throughout all phases with no active matching circuitry, more than 20 dB down. Essentially all power not transmitted to the terminating load is coupled to the plasma. This plasma coupled power is indicated at the top by the difference between the transmitted power and 0 dB. This test case is by no means optimized for plasma coupled power. Modeling of a high power four strap combline for DIII–D, using the F2 straps and power recirculation for enhanced efficiency, projects at least 80% of the power delivered to the plasma throughout variations of up to a factor of eight in the plasma loading,

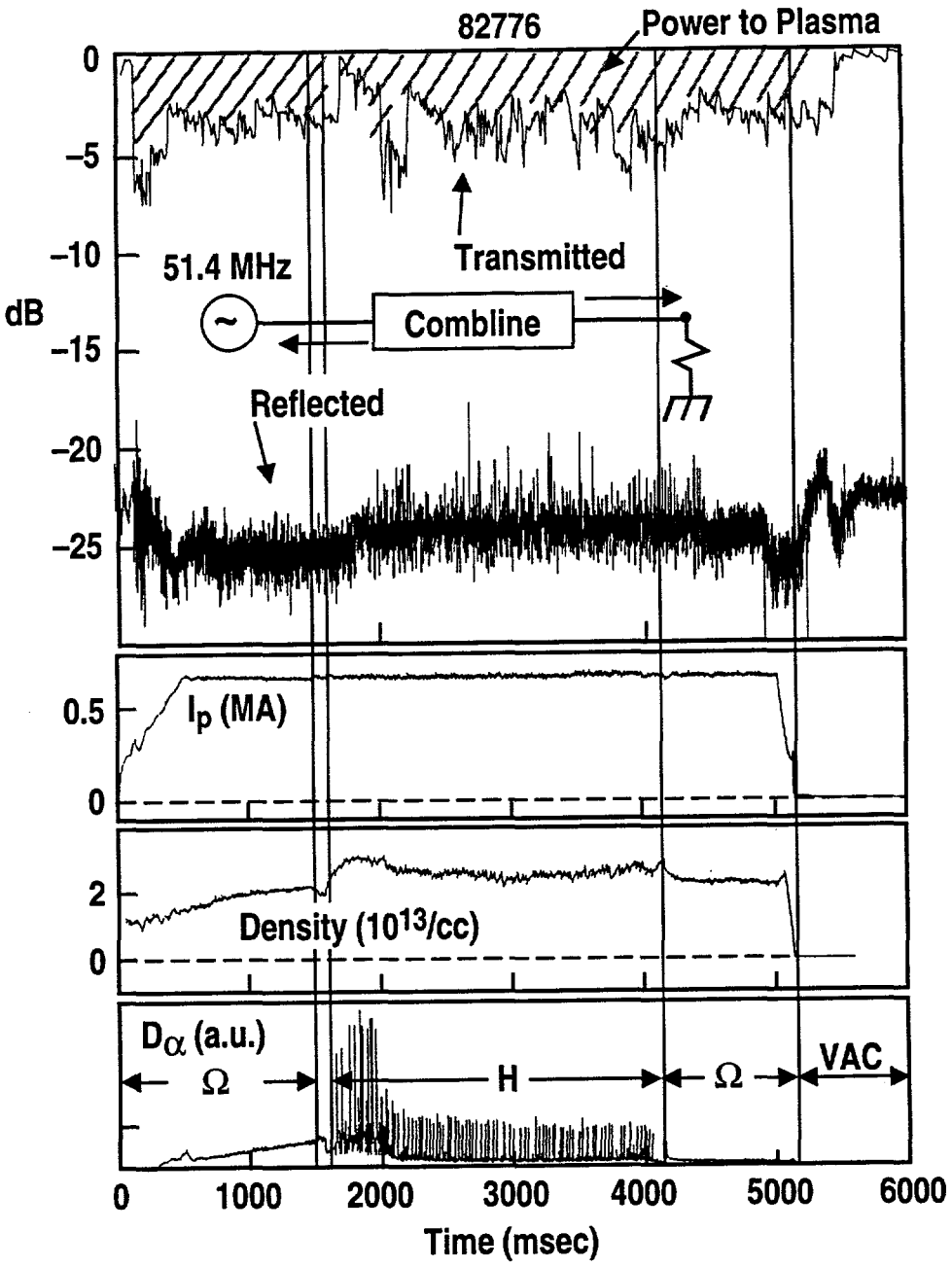

FIGURE 8. Low power reflection and transmission data for F2B antenna in a combline configuration demonstrating a continuous good match. Lower single null discharge with $B_T = 1$ T.

while the power reflected to the generator remains less than 1%. The problem of matching to an arc should be minimal for the combline, but this must be studied.

FAST ION ABSORPTION

There are multiple high harmonic ion gyro resonances in a DIII–D discharge given the generator frequencies and toroidal field strength available, from the third to the twentieth harmonic for D^+ at the extremes of parameter space. A theoretical and experimental effort is underway to understand the amount of fast wave power which is coupled at high resonances to D^+ ions from the neutral beam injectors, for which $k_\perp \rho_i$ is of order 1 to 10, where $k_\perp$ is the perpendicular wavenumber and ρ_i is the ion gyroradius. Relatively few DIII–D experiments to date have used simultaneous high power beam and fast wave injection. This will not be the case for the future AT program. The CQL3D [21] code has been upgraded to include high harmonic resonant ion absorption. Calculations have predicted a greater level of resonant ion absorption than has been seen in the limited number of experiments done as yet.

One experimental technique used is to measure the neutron production rate, dominated by beam-target reactions, with and without fast wave power. Figure 9 shows the decay in the neutron production after termination of the neutral beam pulse. The case with fast wave power at 1 T shows a clear, but small, neutron rate enhancement, which can be modeled with only about 1% of the beam ions accelerated to twice the 60 keV injection energy. The enhancement was not observed with B_T doubled to 2 T, which results in lower harmonic resonances but also smaller $k_\perp \rho_i$. More detailed experiments

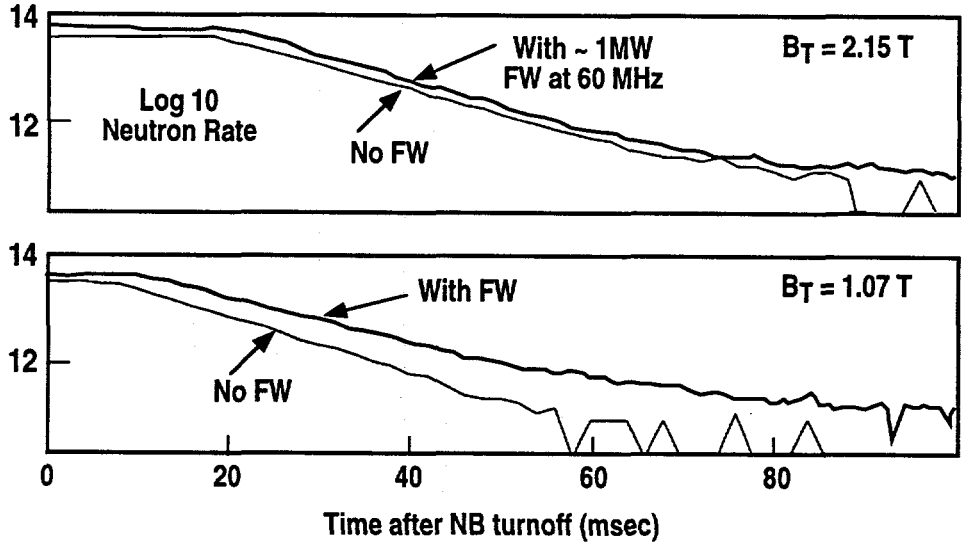

FIGURE 9. Decay of the neutron production rate from D beam-target events after termination of the neutral beam pulse, with and without FW power at 60 MHz. Parameters for this experiment are $P_{FW} = 1$ MW, $P_{NB} = 1.5$ MW, $I_p = 0.75$ MA in double null, and $\bar{n}_e = 2 \times 10^{19}/m^3$.

are planned for the future using fast wave power modulation to measure the amplitude and phase response of the electron temperature profile, which should reveal a loss channel to ion absorption if it is significant.

CONCLUSION

Experiments on DIII–D have demonstrated the physics basis for FWCD. Codes which model the antenna realistically and the coupling to the plasma provide good predictions of the loading and current drive. Coupling uninterrupted high power into AT discharges may require technical innovations and these are being developed. DIII–D is ready to begin the AT phase with FWCD.

ACKNOWLEDGMENTS

This is a report of work supported by U.S. DOE Contracts DE-AC03-89ER51114, DE-AC05-84OR21400, DE-FG03-86ER63266, and W-7405-ENG-48.

REFERENCES

[1] P.A. Politzer *et al.*, "Development of a Tokamak Plasma Optimized for Stability and Confinement," to be published in *Proc. of 6th Int. Conf. on Plasma Physics and Contr. Nucl. Fusion, Toki, Japan*, 1995.
[2] A.D. Turnbull *et al.*, Phys. Rev. Lett. **74**, 718 (1995).
[3] P.A. Politzer *et al.*, Phys. Plasmas **1**, 1545 (1995).
[4] L.L. Lao *et al.*, Phys. Rev. Lett. **70**, 3435 (1993).
[5] J.R. Ferron *et al.*, Phys. Fluids B **5**, 2532 (1993).
[6] R. Majeski *et al.*, Phys. Rev. Lett. **73**, 2204 (1994).
[7] R. Majeski *et al.*, "Mode Conversion Experiments on TFTR," this conference.
[8] C.C. Petty *et al.*, "Fast Wave Current Drive in DIII–D," to be published in *Proc. 15th Int. Conf. on Controlled Fusion and Plasma Physics, Madrid*, 1994.
[9] R.I. Pinsker *et al.*, in *Plasma Physics and Controlled Nuclear Fusion Research* (Proc. 14th Int. Conf. Würzburg, 1992), Vol. 1, p. 109.
[10] R. Prater *et al.*, Plasma Phys. and Contr. Fusion **35**, A53 (1993).
[11] R.H. Goulding *et al.*, in *Proc. 9th Top. Conf. on RF Power in Plasmas, Charleston, South Carolina*, 1991, p. 287.
[12] D.J. Taylor *et al.*, in *Proc. 14th IEEE/NPSS Symp. on Fusion Engineering, San Diego, California*, 1991, Vol. 1, p. 98.

[13] R.I. Pinsker *et al.*, "30–60 MHz, FWCD System on DIII–D: Power Division, Phase Control, and Tuning for a Four-Element Antenna Array," *ibid.*, Vol. 1, p.115.
[14] C.C. Petty *et al.*, Phys. Rev. Lett. **69**, 298 (1992).
[15] J.S. deGrassie *et al.*, in *Proceedings of the 15th IEEE/NPSS Symposium on Fusion Engineering, Hyannis, Massachusetts*, 1993, Vol. 2, p. 1073.
[16] F.W. Baity *et al.*, in *Proc. 10th Top. Conf. on RF Power in Plasmas, Boston, Massachusetts*, 1993, p. 343.
[17] C.B. Forest *et al.*, Phys. Rev. Lett. **73**, 2444 (1994).
[18] W. Arnold *et al.*, "Progress in the Development of an Automatic Impedance Matching Network for ICH," this conference.
[19] C.P. Moeller *et al.*, in *Proc. 10th Top. Conf. on RF Power in Plasmas, Boston, Massachusetts*, 1993, p. 323.
[20] D.A. Phelps *et al.*, "The First Demonstrating of Traveling Wave Antenna (TWA) Performance in a Tokamak and Relevance to JFT–2M," this conference.
[21] S.C. Chiu *et al.*, "Interaction of Fast Waves with Ions," this conference.
[22] H. Ikezi *et al.*, "Fast Wave Propagation Studies in DIII–D, this conference.
[23] J.H. Lee *et al.*, "Fast Wave Electric Field Measurements Using Reflectometry on DIII–D," this conference.
[24] K.W. Kim *et al.*, Rev. Sci. Instrum. **66**, 1229 (1995).
[25] R.I. Pinsker *et al.*, "Direct Electron Heating with Directional Fast Wave Launch on DIII–D," this conference.
[26] E.F. Jaeger *et al.*, "Fast Wave Current Drive Modeling Using the Combined RANT3D and PICES Codes," this conference.
[27] D.A. D'Ippolito *et al.*, Phys. Fluids B **5**, 3603 (1993).
[28] G.L. Jackson *et al.*, J. Nucl. Mater. **196-198**, 236 (1992).
[29] F.W. Baity *et al.*, "Commissioning of the Long-pulse Fast Wave Current Drive Antennas for DIII–D," this conference.
[30] T. Luce *et al.*, in *Proc. 9th Top. Conf. on RF Power in Plasmas, Charleston, South Carolina*, 1991, p. 271.
[31] T.K. Mau *et al.*, in *EPS Top. Conf. on RF Heating and Current Drive of Fusion Devices, Brussels, Belgium*, 1992, p. 181.
[32] H. St. John *et al.*, in *Plasma Physics and Controlled Nuclear Fusion Research* (Proc. 15th Int. Conf. Lisbon, Spain), 1993, Vol. 1, p. 99.
[33] C.B. Forest *et al.*, "Experimentally Determined Profiles of Fast Wave Current Drive on DIII–D," this conference.
[34] K. Kupfer *et al.*, Phys. Plasmas **1**, 3915 (1994).
[35] T.J. Wade *et al.*, in *Proc. 14th IEEE/NPSS Symp. on Fusion Energy, San Diego*, 1991, Vol. 2, p. 902.
[36] J.S. deGrassie *et al.*, in *Proc. 17th Symp. on Fusion Technology, Rome, Italy*, 1992, Vol. 1, p. 457.
[37] For a related concept, see G. Bosia and J. Jacquinot in *Proc. of the IAEA Technical Committee Mtg. on FWCD in Reactor Scale Tokamaks, Arles*, 1991, p. 471.